Determination of the Orientational Distribution and Orientation Factor for Transfer between Membrane-Bound Fluorophores using a Confocal Microscope

Ben Corry,* Dylan Jayatilaka,* Boris Martinac,[†] and Paul Rigby[‡]

*School of Biomedical, Biomolecular and Chemical Sciences, [†]School of Medicine and Pharmacology, and [‡]Biomedical Imaging and Analysis Facility, The University of Western Australia, Crawley, Australia

ABSTRACT   Orientational fluorophores have been a useful tool in physical chemistry, biochemistry, and more recently structural biology due to the polarized nature of the light they emit and that fact that energy can be transferred between them. We present a practical scheme in which measurements of the intensity of emitted fluorescence can be used to determine limits on the mean and distribution of orientation of the absorption transition moment of membrane-bound fluorophores. We demonstrate how information about the orientation of fluorophores can be used to calculate the orientation factor κ^2 required for use in FRET spectroscopy. We illustrate the method using images of AlexaFluor probes bound to MscL mechanosensitive transmembrane channel proteins in spherical liposomes.

INTRODUCTION

Fluorophores are generally complex molecules that, when illuminated with polarized light, emit polarized fluorescence. This is a consequence of their containing dipole moments, known as the absorption and emission transition moments, which form axes along which light is absorbed and emitted. This fact has made measurements of the polarization of fluorescence an important tool. Measurements of the change in polarization of light between absorption and emission reveal the angular rotation the fluorophore undergoes between these events. Similarly, the polarization anisotropy measured from an ensemble of molecules can be used to determine the rotational freedom of the probes. Because the rotational motion of the fluorophores is dependent on the viscosity of its environment and the motion of any molecule to which it is attached, measurements of fluorescence polarization or anisotropy have long provided a useful tool in biochemical research, enabling, for example, the dynamics and supramolecular structure of membranes to be studied (1,2).

Determining the actual orientations of the transition moments of fluorophores in a sample has been a difficult proposition. The angles between absorption and emission transition moments can be determined from anisotropy spectra (3) and the orientation of the moments within the molecule can be obtained in ordered systems such as crystals or stretched films (4,5). It would be of particular interest, however, to be able to determine the orientations of fluorophore transition moments relative to a host molecule to which they are attached, such as when they are bound to proteins or lipids. Determining such orientations would assist in understanding the relative geometry of molecular samples; changes in the

rotational freedom would signal changes in the environment surrounding the fluorophores, and, as noted below, would allow accurate distance measurements using resonance energy transfer.

As noted by Dale et al. (6), experimental techniques to measure the orientation of fluorophores relative to the host molecule were not available in the past. But in the last 20 years a technique has been developed in macroscopically ordered systems where many fluorophores adopt the same orientation relative to a membrane, fiber, or film. Using the original suggestion of van der Meer et al. (7) and elaborated by van Gurp et al. (8), it is possible to relate the fluorophore orientation to the intensity of light emitted by fluorophores with polarizations parallel and perpendicular to the polarization of the incident light. To our knowledge, this technique has only been applied a handful of times. It has been used to determine the orientation of fluorophores attached to cross links in muscle fibers (9,10), to estimate the orientation of fluorophores linked to integral membrane proteins (11) and membrane-bound fluorophores (12), as well as the orientation of transition moments in a green fluorescent protein held rigidly within a larger protein complex (13).

In recent years, information on the orientation of fluorophores has begun to be determined in single molecule experiments (14,15). We are not aware of any such experiments that aim to simultaneously measure the mean fluorophore orientation as well as its angular distribution. However, these techniques have been used to follow the rotation of individual fluorophores assuming a rigid orientation (16) or to determine rotational correlation times (17).

An application where information on the orientation of transition moments is particularly important is in fluorescence resonance energy transfer or FRET. In this process, energy is transferred from one fluorophore called the donor, to another, the acceptor, in a nonradiative manner (18–20).

The likelihood of this occurring and thus, the fraction of energy that is transferred, is related to the distance between the fluorophores, and so this technique is useful for measuring intersite distances and conformational changes within fluorophore-labeled macromolecules (3,9,21).

One complication in studies using FRET, however, is that the efficiency of energy transfer is also dependent on the relative orientations of the transition moments of the donor and acceptor fluorophores. When the transition moments are aligned, energy transfer is more likely than when they are not. In particular, the efficiency of energy transfer between two fluorophores is given by (3,19)

$$E = \frac{1}{1 + \left(\dfrac{r}{R_0}\right)^6}, \qquad (1)$$

in which r is the separation of the fluorophores and R_0 is a characteristic, or Förster distance specific to the fluorophore pair. The Förster distance itself is related to the relative orientation of the transition moments through a term commonly referred to as the orientation factor or simply κ^2, with $R_0^6 \propto \kappa^2$ (19).

To calculate distances between fluorophores undergoing resonance energy transfer, a value for κ^2 must be known. If the fluorophores are spheres (such as the lanthanides), or rapidly diffuse through all possible orientations over the timespan of energy transfer, then a dynamic average value of 2/3 can be used (19,22). In many cases these conditions do not apply, although this average value is still often used for simplicity. The use of this value in general situations has been long debated (see for example (6,22)), and although it yields reasonable results in many situations, it is at best an approximation whose validity can only be determined by comparison with distance measurements obtained from other means such as from x-ray diffraction. The value of κ^2 can vary between 0 and 4, and although the value can contain a host of useful information about the system being studied, in most practical situations it is ''at best a nuisance and at worst an insurmountable problem'' (22). Ideally, therefore, a mechanism for experimentally measuring its value is desirable.

One technique for deducing upper and lower bounds of the average value of κ^2 from anisotropy measurements taken over time periods shorter than the transfer time has been developed (6,23–25) (summarized in (19)). However, as noted by Dos Remedios and Moens (22), the uncertainties calculated in this way can often be large, comparable to the Förster distance R_0 itself. This technique has also been extended to estimate the effective orientation factor directly from anisotropy measurements, assuming that energy transfer occurs in a steady-state manner (26). Another approach is to measure distances using FRET for a system in which the fluorophore separation is already known, and work backward to the orientation factor (27,28). Although this approach has been very useful for demonstrating the validity of FRET dis-

tance measurements, it is obviously of little use as a means of determining the value of the orientation factor in systems in which distances have not yet been measured.

This article is divided into two major sections after Materials and Methods. In the first, Limits on Fluorophore Orientations, we show how the intensity of fluorescence from membrane-bound fluorophores, such as those obtained in confocal microscope images, can be used to place limits on the orientation of the absorption dipole moments. This technique is demonstrated by calculating limits on the orientation of AlexaFluor dyes attached to transmembrane channels. This technique differs from others in that measurements of polarization or anisotropy are not required. In the second major section, Calculating the Orientation Factor, κ^2, for Transfer between Fluorophores with Known Orientational Distributions, we demonstrate how this information on the mean orientation and orientational distribution of fluorophores can be used to calculate the value of the orientation factor, κ^2, for use in measurements of resonance energy transfer between fluorophores. We show that the value of κ^2 will depend on whether the fluorophores are bound together in a particular configuration or independent from one another, and we calculate values of κ^2 for the limiting orientations of the AlexaFluor probes determined previously.

MATERIALS AND METHODS

Fluorescent labeling and imaging of membrane proteins

The images shown in Fig. 4 are of a fluorescently labeled integral membrane protein, the MscL mechanosensitive channel, reconstituted into membrane liposomes.

The native MscL protein contains no cysteine residues, so to label specific sites cysteine residues were introduced at desired locations. In this case, the amino-acid substitution M42C was made. Site-directed cysteine mutants of MscL were cloned into a pQE-32 expression vector (Qiagen, Venlo, The Netherlands) as *Bam*HI-*Sal*I fragments. The encoded MscL proteins were then expressed in *Escherichia coli* with a 6×His-tag attached and purified using the Ni-NTA affinity chromatography as previously described (29). The detergent-solubilized and purified MscL mutant protein was labeled with a mixture of AlexaFluor488 maleimide and AlexaFluor568 maleimide that selectively binds to the cysteine residues. The fluorescent dyes were mixed in equal concentration with the purified protein at 4°C and left overnight. The excess dye was then removed by dialysis by placing a dialysis bag with the labeled protein in a large volume (5–6.l) of detergent-containing buffer. The concentrated labeled protein was reconstituted into artificial phosphatidylcholine liposomes using previously established methods (30).

Liposomes were examined on a BioRad MRC1000/1024 UV laser scanning confocal microscope (BioRad, Hercules, CA) using a Nikon PlanApo 60× NA 1.2 water immersion objective (Nikon, Melville, NY). The AlexaFluor488 probe was excited with the 488-nm laser line from an argon laser and emission detected through a 522/35nm bandpass filter while the AlexaFluor568 probe was excited with the 543-nm line from a green helium neon laser with emission detected through a 585-nm longpass filter. Images were analyzed using Image J (National Institutes of Health, Bethesda, MD). The polarization direction of the laser light at the sample was determined by rotating a polarizing filter at the location of the sample to achieve the maximum transmitted light.

LIMITS ON FLUOROPHORE ORIENTATIONS FROM EMITTED INTENSITIES

Relationship between fluorophore orientation and intensity

When the absorption transition moment of the fluorophore is aligned with the direction of polarization of the incoming light, the chance of the fluorophores being excited is a maximum, and thus (over timescales greater than the lifetime of the excited fluorophore) the emitted intensity from the fluorophore will be large. On the other hand, when the orientation of the fluorophore is perpendicular to the polarization of the exciting light, the fluorophore will not be excited and the re-emitted intensity will be zero.

Specifically, the intensity of the emitted light from an (isolated) fluorophore with absorption dipole-oriented at angle β to the polarization of the incident light source is given by

$$I(\beta) = I_0\cos^2\beta, \tag{2}$$

where I_0 is the intensity of the emitted light when the fluorophore transition moment and the polarization of the incident light are aligned.

In most situations, fluorophores are not held at a fixed orientation, but rather have some degree of freedom in their orientation. When the fluorophores are completely free to rotate, they will have random orientations and the average emitted intensity will be given by the average over all orientations with the appropriate geometric factor, $\sin\beta$, included, as

$$\langle I \rangle = \frac{I_0 \int_0^{\pi/2} d\beta \cos^2\beta \sin\beta}{\int_0^{\pi/2} d\beta \sin\beta} = \frac{I_0}{3}. \tag{3}$$

Emitted intensity of macroscopically ordered fluorophores

In many situations, the fluorophores may be neither completely free, nor held at a fixed orientation, but will have a distribution of orientations relative to a host molecule. If many such fluorophores all share a distribution relative to a scaffold then it is possible to determine the mean orientation and distribution of the fluorophores by measuring either the intensity or polarization of the emitted light.

In this article, we are particularly interested in fluorophores attached to membrane proteins which themselves are embedded within a membrane that forms a (roughly) spherical liposome. However, the techniques we use here could also be applied to fluorophores oriented relative to any form of fiber or film, with suitable modification. In our case, the orientation of both the fluorophore relative to the membrane, and the membrane relative to the polarization of the exciting light, will influence the intensity of the emitted light.

To calculate the average emitted intensity of our fluorophore, we first need to be able to express the orientation of the absorption dipole in terms of the angle between it and the polarization of the exciting light. Since our fluorophore is attached to a protein which is itself embedded in the liposome membrane, we need to introduce a few additional angles (see Fig. 1). We set the polarization direction of the illuminating light to lie along the x axis (the light travels down the z axis). The angle of the membrane normal to the mean fluorophore orientation is set to be α. Likewise, the angle of the membrane normal to the x axis is set to be γ. We assume that the membrane normal always lies in the x-y plane. This can be arranged in the experiment by recording images at the equator of the roughly spherical liposomes. We allow the fluorophore to adopt an angle ψ from its mean (time- and ensemble-averaged) orientation. The probability that it adopts this angle ψ is assumed to be described by a
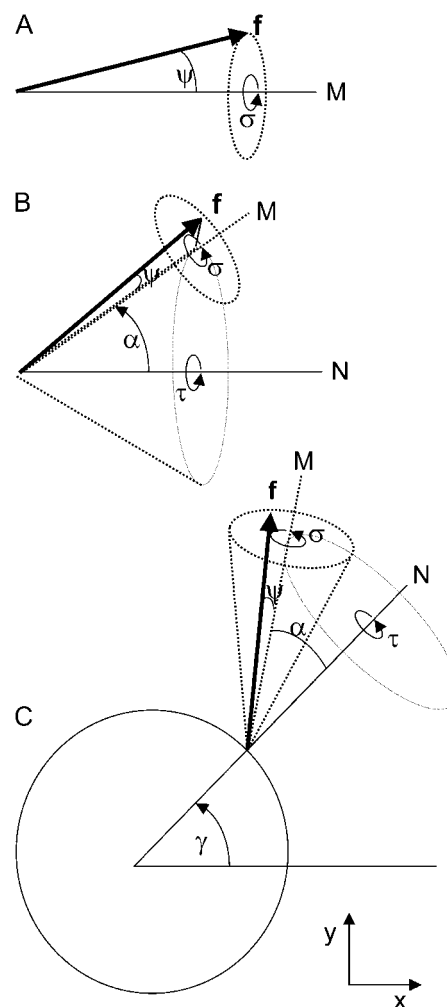

FIGURE 1   The coordinates of an absorption transition dipole relative to the polarization of the illuminating light for membrane-bound fluorophores. The general coordinates of the dipole vector $\mathbf{f}^a$ can be built from successive rotations. First we take the dipole to lie at angle ψ from the mean orientation (M) with a twist of σ about this mean (A). Next we take the mean orientation to lie at angle α from the membrane normal (N) with a twist of τ (B). Finally, the membrane normal itself is rotated by angle γ from the polarization direction of the incident light (x axis) (C).

distribution $g(\psi)$, which is independent of the twist-angle σ about the mean orientation. Finally, the mean orientation of the fluorophore itself is allowed to twist around the membrane normal by an angle τ. This allows for the fact that the host protein molecule can also twist on its axis within the membrane.

The general absorption dipole vector $\mathbf{f}^{a}$, shown in Fig. 1 C, can be determined by taking an initial vector (representing the fluorophore dipole relative to its mean orientation) and performing four rotations as illustrated schematically in Fig. 1, A–C: a rotation of angle σ about the x axis, a rotation of α about the z axis, a rotation of angle τ about the x axis, and finally a rotation of angle γ about the z axis:

$$\mathbf{f}^{a} = \mathrm{rot}_{z}(\gamma)\,\mathrm{rot}_{x}(\tau)\,\mathrm{rot}_{z}(\alpha)\,\mathrm{rot}_{x}(\sigma) \begin{pmatrix} \cos\psi \\ \sin\psi \\ 0 \end{pmatrix}$$

$$= \begin{pmatrix} \cos\gamma(\cos\alpha\cos\psi - \sin\alpha\cos\sigma\sin\psi) \\ -\sin\gamma\cos\tau(\sin\alpha\cos\psi + \cos\alpha\cos\sigma\sin\psi) \\ + \sin\gamma\sin\tau\sin\sigma\sin\psi \\ \\ \sin\gamma(\cos\alpha\cos\psi - \sin\alpha\cos\sigma\ \sin\psi) \\ + \cos\gamma\cos\tau(\sin\alpha\cos\psi + \cos\alpha\cos\sigma\sin\psi) \\ -\cos\gamma\sin\tau\sin\sigma\sin\psi \\ \\ \sin\tau(\sin\alpha\cos\psi + \cos\alpha\ \cos\sigma\sin\psi) \\ + \cos\tau\sin\sigma\sin\psi \end{pmatrix} . \quad (4)$$

Now the angle between the fluorophore vector and the laser light, β, is given by

$$\cos\beta = \mathbf{f}^{a} \cdot \mathbf{x}$$
$$= \cos\gamma(\cos\alpha\cos\psi - \sin\alpha\cos\sigma\sin\psi)$$
$$- \sin\gamma\cos\tau(\sin\alpha\cos\psi + \cos\alpha\cos\sigma\sin\psi)$$
$$+ \sin\gamma\sin\tau\sin\sigma\sin\psi. \quad (5)$$

The average emitted intensity is the average of $\cos^{2}\beta$ over the angles σ, τ, and ψ, again with the geometric factor included, and this time also including the distribution function $g(\psi)$, as

$$\langle I \rangle = \frac{I_0 \int_0^{\pi/2} d\psi \int_0^{2\pi} d\tau \int_0^{2\pi} d\sigma \cos^2\beta\, g(\psi)\sin\psi}{\int_0^{\pi/2} d\psi \int_0^{2\pi} d\tau \int_0^{2\pi} d\sigma\, g(\psi)\sin\psi}. \quad (6)$$

Substitution of the expression for $\cos\beta$ in the above equation, performing the integrations, and simplifying, leads to

$$\langle I \rangle = \frac{I_0}{4}\left[(3\cos^2\alpha - 1)(3\cos^2\gamma - 1)\left(u - \frac{1}{3}\right) + \frac{4}{3} \right], \quad (7)$$

where the quantity u represents a measure of the orientational freedom of the fluorophore and is defined as

$$u = \frac{\int_0^{\pi/2} d\psi \cos^2\psi \sin\psi\, g(\psi)}{\int_0^{\pi/2} d\psi \sin\psi\, g(\psi)}, \quad \text{where} \quad 0 \leq u \leq 1. \quad (8)$$

We can rewrite this expression to explicitly show the dependence on the angle γ,

$$\langle I \rangle = \frac{I_0}{4}\left[3B\cos^2\gamma - B + \frac{4}{3} \right], \quad (9)$$

where

$$B = (3\cos^2\alpha - 1)\left(u - \frac{1}{3}\right). \quad (10)$$

It is clear that the emitted intensity $\langle I \rangle$ will vary sinusoidally as the membrane is rotated relative to the incident light (i.e., as γ is varied). Since we are interested in proteins embedded in spherical membrane liposomes, the curvature of the membrane naturally produces the full range of γ. If the membrane was not curved in this way, then the angle between the membrane and the polarization of the incident light could be varied by simply rotating the sample. In any case, one can fit the observed intensity variation to obtain the parameter B. The details of obtaining the B parameter, as well as extracting limits on the possible values of α and u, are discussed later.

At what angles do the maxima and minima of the intensity occur? Differentiating Eq. 9 yields

$$\frac{\partial \langle I \rangle}{\partial \gamma} = -\frac{3I_0}{2} B \cos\gamma \sin\gamma. \quad (11)$$

Setting this to zero, it can be seen that for any given fluorophore orientation and distribution (i.e., any values of α and u) the intensity has either a maximum or minimum value at $\gamma = 0$ and $\pi/2$. Whether $\gamma = 0$ is a maximum or minimum value depends on the value of the angle α between the mean fluorophore orientation and the membrane normal. For small values of α, the intensity is a maximum at $\gamma = 0$, whereas for large values it is a minimum. This can be seen in Fig. 2 A, where the average intensity is plotted at $\gamma = 0$ and $\gamma = \pi/2$ against the value of α. Notably, $\gamma = 0$ changes from a maximum to a minimum at the so-called magic-angle, $\cos\alpha = 1/\sqrt{3}$, $\alpha \approx 54.7°$.

The relationship between the average intensity and the angles α and γ is plotted in more detail in Fig. 2 B where the intensity is plotted for the full range of angles, assuming that the fluorophores always lie along the mean orientation (i.e., $u = 1$, see Fixed Fluorophores, below).

Limiting cases for the average intensity

So far we have not assumed any form for the distribution of fluorophores about the mean value. To help visualize the situation and to check the correctness of our results it is worth considering the simplest axially symmetric distribution function: a uniform distribution in a cone of half-angle ψ_0,
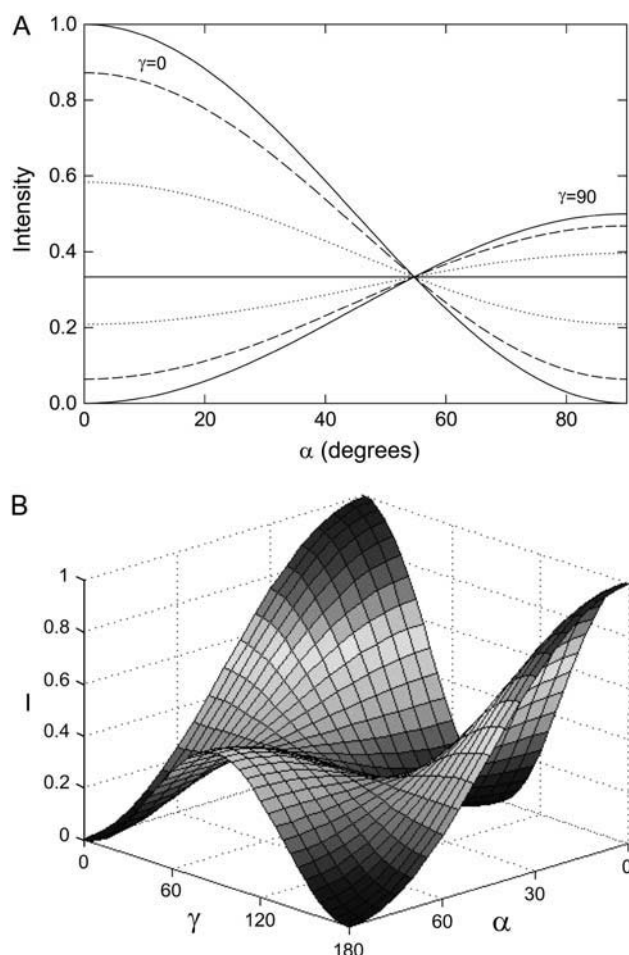
$u = 1/3$ (since $\psi_0 = \pi/2$ in Eq. 13), and Eq. 10 shows that $B = 0$. Equation 9 then gives $I = I_0/3$ in agreement with Eq. 3.

Fixed fluorophores

If the fluorophores have a fixed orientation relative to the membrane, then $u = 1$ ($\psi_0 = 0$ in Eq. 13). Thus, $B = (2/3)(3\cos^2\alpha - 1)$. Consider now the maxima and minima of $\langle I \rangle$. If $\gamma = 0$, then

$$\langle I \rangle_{\gamma=0} = \frac{I_0}{2}\left[B + \frac{2}{3}\right] = I_0\cos^2\alpha. \tag{14}$$

On the other hand, if $\gamma = \pi/2$, then

$$\langle I \rangle_{\gamma=\pi/2} = \frac{I_0}{4}\left[\frac{4}{3} - B\right] = \frac{I_0}{2}(1 - \cos^2\alpha). \tag{15}$$

Two further subcases are of interest:

1. Fluorophores are aligned with the membrane normal: In this case, $\alpha = 0$ and

$$\langle I \rangle_{\gamma=0} = I_0, \quad \langle I \rangle_{\gamma=\pi/2} = 0 \tag{16}$$

2. Fluorophores are perpendicular to the membrane normal: In this case, $\alpha = \pi/2$ and

$$\langle I \rangle_{\gamma=0} = 0, \quad \langle I \rangle_{\gamma=\pi/2} = I_0/2. \tag{17}$$

Note that in the second case the intensity is not I_0, as the absorption dipole is still averaged over the protein twist-angle τ.

FIGURE 2 The dependence of the emitted intensity, $\langle I \rangle$, on the angle between the transition dipole and the membrane normal (α) and the membrane normal to the incident polarization (γ). (A) The intensity is plotted at $\gamma = 0$ (*lines descending* to the *right*) and $\gamma = 90°$ (*lines ascending* to the *right*) for all α and four values of u. The orientational freedom as described by the uniform distribution in a cone is $\psi_0 = 0$ ($u = 1$) (*solid lines*); $\psi_0 = 30°$ ($u = 0.87$) (*dashed line*); $\psi_0 = 60°$ ($u = 0.58$) (*dotted line*); and $\psi_0 = 90°$ ($u = 1/3$) (*horizontal solid line*). (B) The intensity is plotted for all possible values of α and γ assuming $u = 1$.

$$g(\psi) = \begin{cases} 1 & \text{for} \quad 0 < \psi < \psi_0 \\ 0 & \text{for} \quad \psi > \psi_0 \end{cases}. \tag{12}$$

In this case, $\psi_0 = 0$ implies rigidly fixed fluorophores, while $\psi_0 = \pi/2$ implies completely free fluorophores with no mean orientation. For this distribution model, u can be evaluated explicitly to be

$$u = \frac{1}{3}(1 + \cos\psi_0 + \cos^2\psi_0). \tag{13}$$

Randomly oriented fluorophores

If the fluorophores have complete orientational freedom, we expect to get an intensity independent of γ and α. In this case,

Obtaining the value of the *B* parameter

The expression for $\langle I \rangle$, Eq. 9, contains the parameter I_0, which will depend upon a number of unknown quantities such as the intensity of the incident light, the volume and density of illuminated fluorophores, and the extinction coefficients, as well as the efficiencies and settings of the detector. For this reason we must consider only ratios of intensities so that I_0 can be eliminated. This can be done by taking the ratios at the points of maximum and minimum intensity, i.e.,

$$R = \frac{\langle I \rangle_{\gamma=0}}{\langle I \rangle_{\gamma=\pi/2}} = \frac{-2(3B + 2)}{3B - 4}, \tag{18}$$

or even better, by taking a ratio across the entire range of γ,

$$R(\gamma) = \frac{\langle I \rangle(\gamma)}{\langle I \rangle(\gamma + \pi/2)} = \frac{3B\cos^2\gamma - B + 4/3}{3B\cos^2(\gamma + \pi/2) - B + 4/3}, \tag{19}$$

which can be fitted to the experimental data to yield a value for B.

How to determine limits on fluorophore orientation from a confocal image of the liposome

Ideally, we would like to be able to determine values of α and u from a plot relating the emitted intensity $\langle I \rangle$ to the angle of the membrane normal γ. However, as is clear from Eq. 9, there is only one independent variable, B, in the expression for $\langle I \rangle$. Clearly, many different combinations of mean orientation and angular distribution may lead to the same emitted intensity. Thus, even if experimental data can be perfectly fitted, the best that can be achieved is a relationship between α and u, not explicit values for these quantities.

Although explicit values of α and u cannot be determined, a range of allowed values can be. First, one can obtain immediate qualitative information about the angle α from the observation of whether $\langle I \rangle$ is a maxima or minimum at $\gamma = 0$. In the former case, α must be $<54.7°$, whereas in the latter case, α is larger than the magic-angle. Second, the measured value of B puts some constraints on the allowed values of α and u. The angle α must be $<90°$, whereas the value of the parameter u must be between zero and one. Thus, plotting Eq. 10 with the measured value of B yields a curve in the α–u plane from which one can establish allowed limits on these quantities. In Fig. 3, a series of contours of B have been made as a function of α and u to allow such a range to be obtained.

A closer examination of Fig. 3 shows that there are four distinct regions. For each of these regions, explicit formulae for the ranges of the allowed values of α and u can be obtained:

1. At $\gamma = 0$, a maximum (i.e., $\alpha < 54.7°$) and $B > 0$, which implies $u_{min} < u < 1$ and $0 < \alpha < \alpha_{max}$, where

$$u_{min} = \frac{3B + 2}{6}, \; \cos^2\alpha_{max} = \frac{3B + 2}{6}. \tag{20}$$

2. At $\gamma = 0$, a maximum (i.e., $\alpha < 54.7°$) and $B < 0$, which implies $0 < u < u_{max}$ and $0 < \alpha < \alpha_{max}$, where

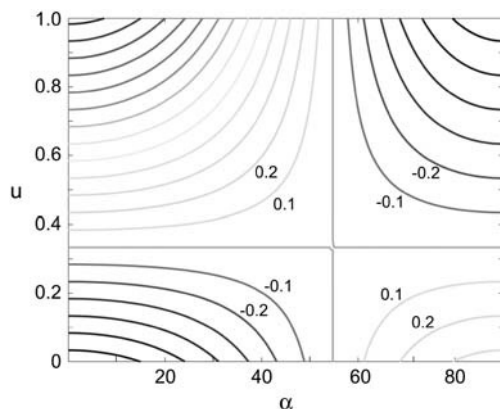$$u_{max} = \frac{3B + 2}{6}, \; \cos^2\alpha_{max} = \frac{1 - 3B}{3}. \tag{21}$$

FIGURE 3 Plot of the observable parameter, B, in terms of the mean fluorophore orientation, α, and orientational freedom, u. Contour intervals of 0.1 are shown.

3. At $\gamma = 0$, a minimum (i.e., $\alpha > 54.7°$) and $B > 0$, which implies $0 < u < u_{max}$ and $\alpha_{min} < \alpha < 90°$, where

$$u_{max} = \frac{1 - 3B}{3}, \; \cos^2\alpha_{min} = \frac{1 - 3B}{3}. \tag{22}$$

4. At $\gamma = 0$, a minimum (i.e., $\alpha > 54.7°$) and $B < 0$, which implies $u_{min} < u < 1$ and $\alpha_{min} < \alpha < 90°$, where

$$u_{min} = \frac{1 - 3B}{3}, \; \cos^2\alpha_{min} = \frac{3B + 2}{6}. \tag{23}$$

Orientation of AlexaFluor probes in membrane liposomes

In Fig. 4, we show two images of a spherical liposome in which MscL mechanosensitive ion channels are embedded that have been labeled with both AlexaFluor488 (AF488) and AlexaFluor568 (AF568) fluorescent dyes. In Fig. 4 A, we show an image taken in the AF568 emission band when the sample is excited with a Helium-Neon 543 nm laser, whereas in Fig. 4 B, we show the same liposome imaged in the AF488 emission band when excited with a Argon 488-nm laser . Thus, Fig. 4 A images the AF568 fluorophores, whereas Fig. 4 B images AF488. Details of the sample preparation and imaging technique can be found in Materials and Methods. It is obvious, particularly in Fig. 4 A, that the intensity of the liposome varies around its circumference.

In this case, the image has been aligned so that the known polarization of the illuminating laser is along the x axis. It is relatively clear from the images in Fig. 4 that the intensity is a maximum when the membrane normal is perpendicular to the direction of polarization of the incident light. That is, the intensity is a maximum at $\gamma = \pi/2$, while it is a minimum at $\gamma = 0$.

In Fig. 5, A and B, we plot the intensity profile along an oval placed over the liposome circumference of the images in Fig. 4, A and B, with the gray line. It can clearly be seen that the liposome has two bright regions and two dim regions offset by 90°. Furthermore, one bright region is slightly more intense than the other, so we also plot the average intensity of the two sides of the liposome by the solid line (this curve therefore repeats every 180°). Assuming a uniform distribution of MscL channel pentamers, the asymmetry in the image intensity is most likely a result of nonuniformity in the membrane forming the liposome. In many cases blebbing of the membrane is apparent and it can be difficult to produce uniform, unilaminar liposomes. Such lack of uniformity is likely to skew the calculations of fluorophore orientations. For this reason, images of many liposomes should be taken and the intensities averaged to gain more reliable results.

To determine information about the orientation of the fluorophores, in Fig. 5 C we plot the normalized intensity of
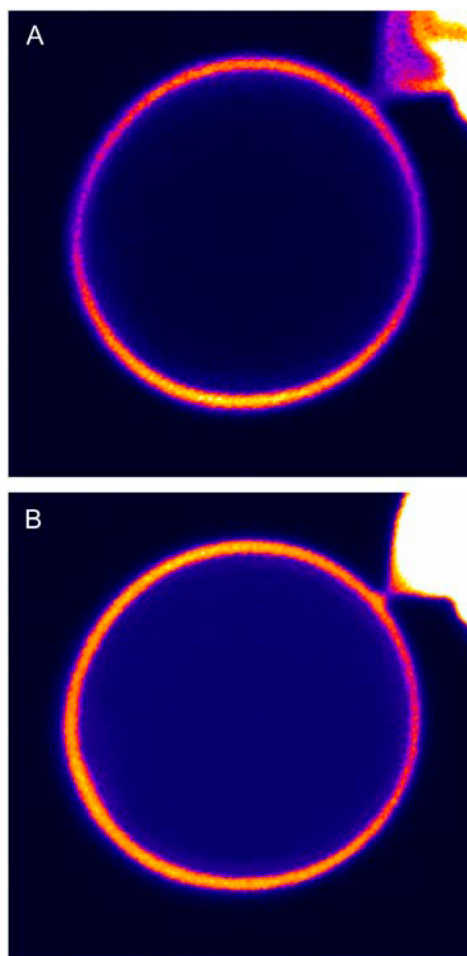
FIGURE 4 Confocal microscope images of membrane-bound fluorophores attached to spherical liposomes. Fluorescence is measured in the emission bands of (A) AlexaFluor568 and (B) AlexaFluor488 fluorophores when excited with a 543- and 488-nm polarized light source, respectively. Fluorophores are bound to an integral membrane protein, the mechanosensitive channel MscL. The polarization of the incident light lies along the x axis.

the images shown in Fig. 4, A and B, obtained by dividing the intensity at every value of γ by the value at $\gamma + \pi/2$. Using Eq. 19 we can fit the data to determine the value of the parameter B. In Table 1 we show the results of this fit for the AF568 and AF488 fluorophores, as well as the limits on the values of α and u determined as described above. Although there is a large range of mean orientations and distribution (i.e., a large range of allowed values of α and u) consistent with our data, placing limits on the range can provide useful information as described in Example Calculation for Fluorophores on a Pentameric Protein. The error values shown for the parameter B only represent the error in fitting the normalized data shown in Fig. 5 C and so does not take into account the fact that one side of the imaged liposome is considerably brighter than the other. Ideally, to obtain accurate results, images of many liposomes should be used and the normalized intensities of each averaged before determining the value of B.
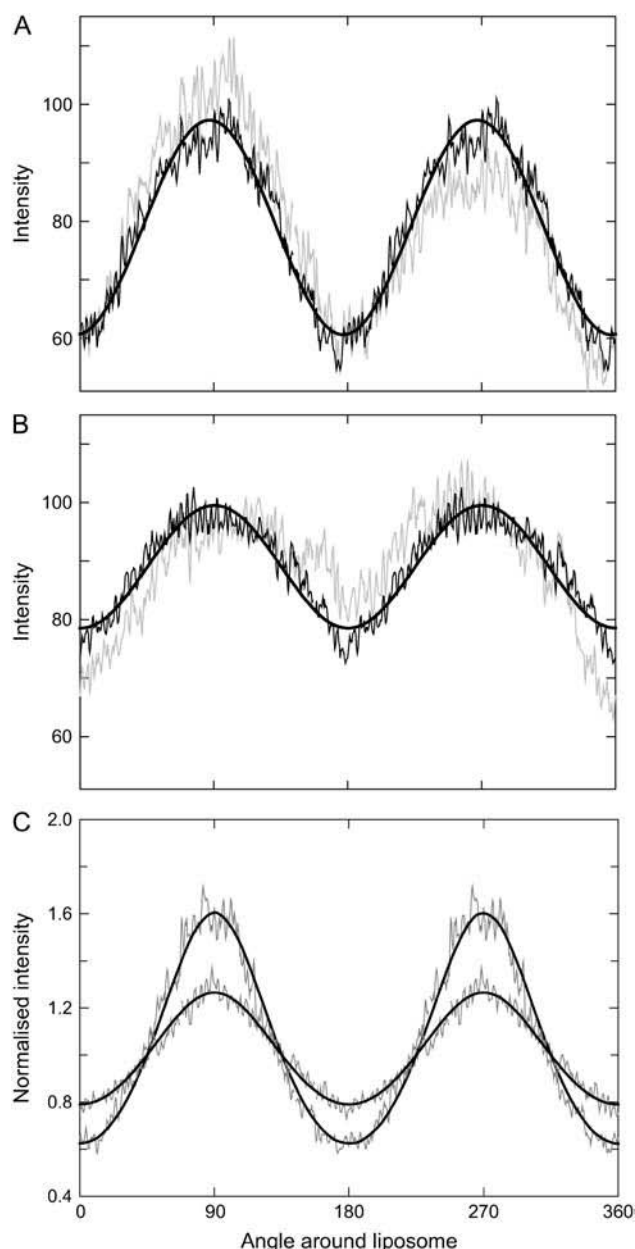
FIGURE 5 Intensity measurements for the images shown in Fig. 4. (A) The intensity measured around the circumference of the liposome starting at the middle right-hand side of the image in Fig. 4 A moving in a clockwise direction around the circumference of the liposome. Raw data is plotted by the shaded line. The average of the two sides of the liposome is plotted in solid representation and fitted by the thick solid line as described in the text. (B) A similar figure as panel A for the second image in Fig. 4. (C) The normalized intensity around the liposome as described in the text. Data for the image in Fig. 4, A and B, are fitted by the thick lines.

Limits on fluorophore orientations from polarization measurements

So far we have discussed how the relative intensity of the emitted light can be used to obtain information about the orientation of fluorophores. It is worth noting that similar

TABLE 1 A summary of results obtained from the images shown in Fig. 4

Measure	AF568	AF488
Maximum intensity	97 ± 1	100 ± 2
Minimum intensity	61 ± 1	79 ± 2
B	-0.192 ± 0.001	-0.100 ± 0.001
$\alpha_{\min}$	$60.8°$	$57.8°$
$\alpha_{\max}$	$90°$	$90°$
$u_{\min}$	0.525	0.433
$u_{\max}$	1.0	1.0

information can be gained from measurements of the polarization of the emission as such measurements may avoid some of the difficulties involved in accurately measuring the intensity of the emission (albeit with the added effort of determining polarization). We can do this if the reorientation of the fluorophores is faster than the lifetime of the excited state, in which case the intensity of light polarized parallel and perpendicular to the incident light (aligned to the x axis) are given by

$$\langle I \rangle_x = \langle (\mathbf{x} \cdot \mathbf{f^a})^2 \rangle \langle (\mathbf{f^e} \cdot \mathbf{x})^2 \rangle = \langle I \rangle \langle (\mathbf{f^e} \cdot \mathbf{x})^2 \rangle$$
$$\langle I \rangle_y = \langle (\mathbf{x} \cdot \mathbf{f^a})^2 \rangle \langle (\mathbf{f^e} \cdot \mathbf{y})^2 \rangle = \langle I \rangle \langle (\mathbf{f^e} \cdot \mathbf{y})^2 \rangle, \quad (24)$$

in which $\mathbf{f^a}$ and $\mathbf{f^e}$ are the absorption and emission dipole vectors. A measure of the polarization of the emitted light can be made as $(\langle I \rangle_x - \langle I \rangle_y)/(\langle I \rangle_x + \langle I \rangle_y)$, which is a function of the unknown parameters α, u, and ϕ as well as the angle between the absorption and emission dipoles (θ) and the angle around the liposome γ, where ϕ is the twist-angle of the emission dipole around the absorption dipole.

Calculating these expressions yields a somewhat complex expression for the polarization that is a function of six variables: γ, α, u, θ, ϕ, and w, another distribution parameter. As α, u, ϕ, and w would typically not be known in any experiment, this expression is less useful than those derived from the total intensity alone (Eq. 9).

There are two cases in which measurements of the polarization of the emitted light can be used to gain information on the orientation of the fluorophores. If the absorption and emission dipoles are known to be roughly co-linear, then $\theta = 0$ and the expression for the polarization becomes

$$\frac{\langle I \rangle_x - \langle I \rangle_y}{\langle I \rangle_x + \langle I \rangle_y} = \frac{6B(2\cos^2\gamma - 1)}{2B + \frac{16}{3}}. \quad (25)$$

Fits of experimental data with this equation can be used to gain a value of the B parameter, and a relationship between the mean orientation and angular distribution of the fluorophores can be determined as before.

Alternatively, if the angle between the absorption and emission dipoles is known to be nonzero, and the molecule can rotate such that all twist-angles ϕ are equally likely; then this twist angle can be averaged out and the expression for the polarization becomes

$$\frac{\langle I \rangle_x - \langle I \rangle_y}{\langle I \rangle_x + \langle I \rangle_y} = \frac{3(3\cos^2\theta - 1)B(2\cos^2\gamma - 1)}{(3\cos^2\theta - 1)B + \frac{16}{3}}, \quad (26)$$

which again can be used to determine the value of the B parameter.

Can an exact distribution of orientations be determined from ensemble measurements?

In the preceding sections we developed a technique for determining a range of mean orientations (α) and distributions (u) for membrane-bound fluorophores. An obvious question is whether exact values of these parameters can be determined rather than just a range. The reason why only a range of values could be determined is that many different mean orientations and distributions can give the same emitted intensity. We examined the possibility of either imaging the liposome away from the equator, or measuring the polarization of the emitted light, using a similar approach to that developed above to avoid this problem. Unfortunately, no extra information can be gained in this way and it appears that it is impossible to determine the exact distribution of fluorophores from such ensemble measurements.

For example, if we image the spherical liposome away from the equator, then the average intensity is given by

$$\langle I \rangle = \frac{1}{4}\left[3\cos^2\xi\cos^2\gamma B - B + \frac{4}{3}\right], \quad (27)$$

in which ξ is the latitude angle away from the equator and the mean orientation and distribution are still linked by the parameter B.

One might also think that additional information about the orientation of the fluorophores could be obtained from measurements of the polarization of the emitted light. But, as discussed in the preceding section, no additional information is derived from this measurement as the mean orientation and distribution are again coupled in the factor B. Indeed, measurements of the polarization of the emitted light are likely to introduce a new degree of uncertainty, because even if the angle between the absorption and emission dipoles is known, the expression for the polarization of the emitted light contains a new unknown: the twist-angle of the emission dipole about the absorption dipole relative to the polarization of the incident light.

Application to single molecule studies

The results derived so far have been aimed at studies of ensembles of macroscopically oriented fluorophores. Given the recent development of single molecule fluorescence investigations, it is worth considering how this method could be applied to examine the orientations of individual fluorophores.

If a single fluorophore is not restrained and the emitted intensity is averaged over a long time period, the same results

derived for the ensemble should be applicable. On the other hand, if the host molecule does not twist significantly within the membrane over the timespan of imaging, or if it is fixed to a surface, the averaging over the twist-angle of the host molecule τ will not apply. In this case, τ will have a single value for a given measurement, and simplifying Eq. 6 without averaging over τ yields

$$\langle I \rangle = \frac{3}{2}(u - 1/3)[\cos^2\tau(\cos^2\gamma - 1)(\cos^2\alpha - 1)$$
$$- \cos\tau \cos\gamma \sin\gamma \cos\alpha \sin\alpha$$
$$+ (\cos^2\gamma \cos^2\alpha - 1)]. \qquad (28)$$

When analyzing a single molecule it is obviously impossible to gain information for the entire range of γ values in a single image as described previously. In this case, the same results can be achieved by either rotating the sample, or rotating the direction of polarization of the incident light as done previously by Adachi et al. (16). By taking a ratio of the intensities at different angles of γ as described for the ensemble case, the results can be uniquely fitted to yield values of τ, and more importantly the mean orientation of the fluorophore relative to the membrane, α. Although the orientational distribution parameter u cannot be determined from this experiment unless accurate absolute intensities are known, if combined with ensemble studies it is, in principle, possible to gain explicit information on both the mean orientation and distribution of the fluorophore. Such single molecule experiments raise the possibility of experimentally determining exact orientation factors for use in FRET studies.

CALCULATING THE ORIENTATION FACTOR, κ^2, FOR TRANSFER BETWEEN FLUOROPHORES WITH KNOWN ORIENTATIONAL DISTRIBUTIONS

One important reason for measuring the orientation of fluorophores is to improve the accuracy of FRET measurements where the relative orientation of the donor emission dipole and acceptor absorption dipole is critical for accurately determining the distance between them. We next show how knowledge of the orientational distribution of fluorophores can be used to calculate the orientation factor κ^2 for energy transfer between fluorophores.

Theory

The value of the orientation factor depends upon the relative orientations of the transition moments of the donor and acceptor fluorophores and the line joining them, $\mathbf{r}$,

$$\kappa^2 = [\mathbf{f}_D^e \cdot \mathbf{f}_A^a - 3(\mathbf{f}_D^e \cdot \mathbf{r})(\mathbf{f}_A^a \cdot \mathbf{r})]^2, \qquad (29)$$

where $\mathbf{f}_D^e$ is the donor emission dipole, and $\mathbf{f}_A^a$ is the acceptor absorption dipole (both normalized to unity).

The orientation factor can be easily calculated if the fluorophores have a known static orientation; however, the task is more difficult if they have a degree of orientational freedom. One must consider the variety of specific orientations that the fluorophores can have as well as the possibility of their changing orientation during the energy transfer process. In many applications it is assumed that the fluorophores have complete dynamic orientational freedom, in which case the value of κ^2 is averaged over all angles and yields a value of 2/3 (19). Occasionally static averages in which the orientation of the fluorophores is assumed not to change during the lifetime of the excited state are also applied, although this approach has been criticized (6,31). It is of interest, however, to calculate the value of κ^2 for the partially constrained distributions discussed previously.

Dale et al. (6) worked out a practical expression for κ^2 in terms of the depolarization of light measured in the FRET experiment. The idea of Dale et al. (6) is explained below, but in our scheme we will not need to perform any polarization measurements.

Fig. 6 A depicts schematically the process of resonance energy transfer. During the lifetime of the excited state of the donor fluorophore, the emission dipole moves from an initial to final orientation ($D_i \rightarrow D_j$). Then, energy transfer takes place to the absorption dipole of the acceptor ($D_j \rightarrow A_i$). Finally, the acceptor absorption dipole moves while the acceptor remains in the excited state ($A_i \rightarrow A_j$), after which emission occurs.

If reorientation of the dipoles is faster than energy transfer, then many possible orientations will be tried out in a transfer period. In this case, the actual situation described above can be approximated by the model depicted in Fig. 6 B. In this model, the dipole of the donor reorients to the mean orientation ($D_i \rightarrow D_x$), and a transfer occurs between fluorophores adopting their mean orientation ($D_x \rightarrow A_x$), followed by a reorientation by the acceptor from its mean to final orientation ($A_x \rightarrow A_j$).

Under these approximate circumstances, Dale et al. (6) showed that the mean value of κ^2 can be simplified to give

$$\langle \kappa^2 \rangle = \kappa^{x2}\langle d_D^x \rangle\langle d_A^x \rangle + \frac{1}{3}(1 - \langle d_D^x \rangle) + \frac{1}{3}(1 - \langle d_A^x \rangle)$$
$$+ \cos^2\theta_D\langle d_D^x \rangle(1 - \langle d_A^x \rangle) + \cos^2\theta_A\langle d_A^x \rangle(1 - \langle d_D^x \rangle). \qquad (30)$$

In this equation, κ^{x2} is an orientation factor defined between the mean orientations of the donor and acceptor; θ_D ad θ_A are the angles between the donor and acceptor transition moments and the line joining the fluorophores; and the depolarization factors are

$$\langle d_D^x \rangle = \frac{1}{2}(3\langle \cos^2\psi_D \rangle - 1), \ \langle d_A^x \rangle = \frac{1}{2}(3\langle \cos^2\psi_A \rangle - 1). \qquad (31)$$

Notice that the depolarization factors are simple functions of the angular distribution parameter u discussed previously since $u \equiv \langle \cos^2\psi \rangle$ (Eq. 8). Thus, if the mean orientation of
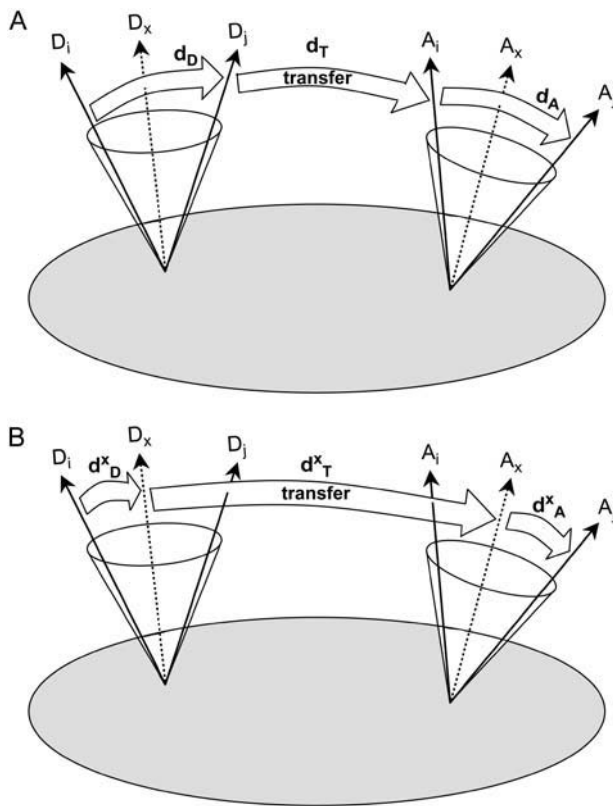
FIGURE 6 Depolarization steps during resonance energy transfer. (A) Depolarization of the incident light can occur by the donor molecule rotating from and initial orientation D_i to a final orientation D_j, during the transfer process if the donor and acceptor transition moments are not perfectly aligned, and by rotation of the acceptor before emission. This depolarization is equivalent to the situation shown (B) where the donor rotates to its mean orientation between absorption and energy transfer, energy transfer arises between fluorophores oriented at their mean positions, and the acceptor rotates to a final orientation.

the fluorophores is known, κ^{x2} can be calculated, while the depolarization factors, and thus $\langle\kappa^2\rangle$, can be determined for a given fluorophore orientation distribution. In our case, since we have already determined limits on the values of the angular and distribution parameters, we will be able to place limits on the value of κ^2 without any further measurements. In particular, from Eq. 10,

$$\langle d_D^x\rangle = \frac{3}{2}\left(\frac{B_D}{\cos^2\alpha_D - 1}\right), \ \langle d_A^x\rangle = \frac{3}{2}\left(\frac{B_A}{\cos^2\alpha_A - 1}\right). \quad (32)$$

Substitution into Eq. 30 shows that $\langle\kappa^2\rangle$ becomes a function of α_D and α_A.

Careful readers will note that the value of the u parameter discussed previously actually involves the absorption dipole moment, whereas the procedure described above involves the emission dipole moment of the donor. These dipoles need not be co-linear. Since the emission and absorption dipoles are usually on the same molecular fluorophore, it seems very reasonable to assume that the u parameters for the absorption and emission dipoles are the same. However, it may not be

reasonable to assume that κ^{x2} can be calculated from the absorption dipole orientation. In the following, we make the co-linear approximation. However, these results can be extended if the angle between the absorption and emission dipoles is known. In this case the emission dipole can be expressed by two additional angles: θ the angle between the absorption and emission dipoles, and ϕ, a twisting of the emission dipole about the absorption dipole in the laboratory frame of reference. If this twist-angle is known, then extending the co-linear results below involves replacing the angle between the absorption dipole and membrane normal with the angle between the emission dipole and the membrane normal, i.e.: $\alpha_D \to \cos^{-1}(\cos\alpha_D\cos\theta - \sin\alpha_D\cos\phi\sin\theta)$. A further simplification exists if one assumes all the twist-angles are equally likely, in which case this angle can be averaged out leaving only the transformation $\alpha_D \to \cos^{-1}(\cos\alpha_D\cos\theta)$.

κ^2 for independent fluorophores

If we know the mean orientation and distribution of two independent fluorophores (i.e., if they are not attached to each other in any given geometry), then we can work out the orientation factor for transfer between them. To do this we orient the coordinates such that the membrane lies in the x-y plane and two fluorophores undergoing energy transfer lie on the x axis but are free to rotate their orientation about the membrane normal (τ) as depicted in Fig. 7 A. We can then generate two dipole vectors for the fluorophores:

$$\mathbf{f}_D = \mathrm{rot}_z(\tau_D)\begin{pmatrix}\sin\alpha_D\\0\\\cos\alpha_D\end{pmatrix} = \begin{pmatrix}\cos\tau_D\sin\alpha_D\\\sin\tau_D\sin\alpha_D\\\cos\alpha_D\end{pmatrix}$$

$$\mathbf{f}_A = \mathrm{rot}_z(\tau_A)\begin{pmatrix}\sin\alpha_A\\0\\\cos\alpha_A\end{pmatrix} = \begin{pmatrix}\cos\tau_A\sin\alpha_A\\\sin\tau_A\sin\alpha_A\\\cos\alpha_A\end{pmatrix}. \quad (33)$$

Now, the average value of the orientation factor for transfer between the mean orientations will be given by averaging over all possible values of τ_D and τ_A:

$$\langle\kappa^{x2}\rangle = \frac{1}{4\pi^2}\int_0^{2\pi}\int_0^{2\pi}\left[(\mathbf{f}_D\cdot\mathbf{f}_A) - 3(\mathbf{f}_D\cdot\mathbf{x})(\mathbf{f}_A\cdot\mathbf{x})\right]^2 d\tau_D\, d\tau_A$$

$$= \frac{1}{4}(5\sin^2\alpha_D\sin^2\alpha_A + 4\cos^2\alpha_D\cos^2\alpha_A). \quad (34)$$

If the fluorophores have a distribution of orientations about the mean, then the depolarization factors are

$$\langle d_D^x\rangle = \frac{3}{2}u_D - \frac{1}{2}, \ \langle d_A^x\rangle = \frac{3}{2}u_A - \frac{1}{2}, \quad (35)$$

and the angles θ_D and θ_A are

$$\cos^2\theta_D = \langle\cos^2\tau_D\sin^2\alpha_D\rangle = \frac{1}{2}\sin^2\alpha_D$$

$$\cos^2\theta_A = \langle\cos^2\tau_A\sin^2\alpha_A\rangle = \frac{1}{2}\sin^2\alpha_A. \quad (36)$$

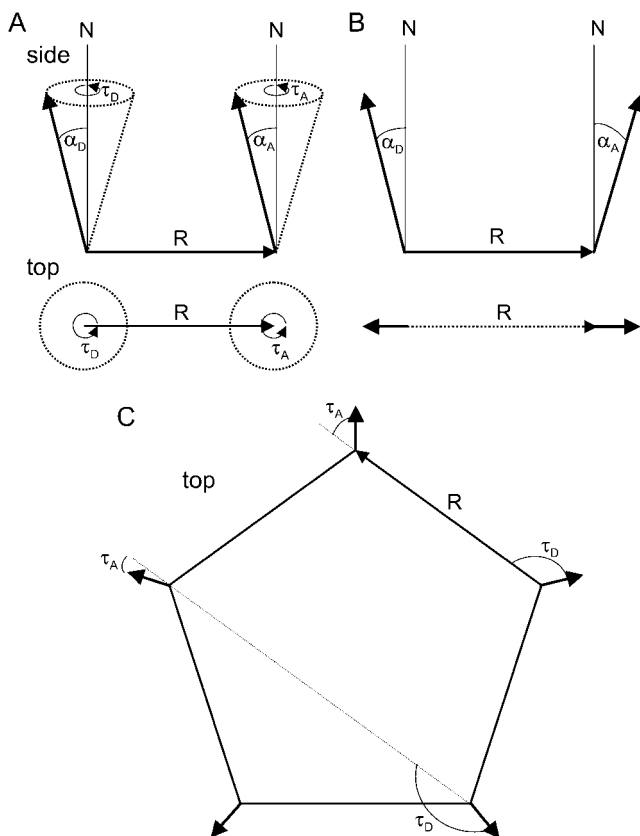FIGURE 7 Diagram showing the angles between fluorophores for calculation of the orientation factor κ^2. (A) Independent fluorophores with mean orientations at α from the membrane normal (N) and twist τ. (B) Situation for fluorophores attached to opposite sides of a symmetric molecule. (C) Situation for fluorophores attached in a pentamer.
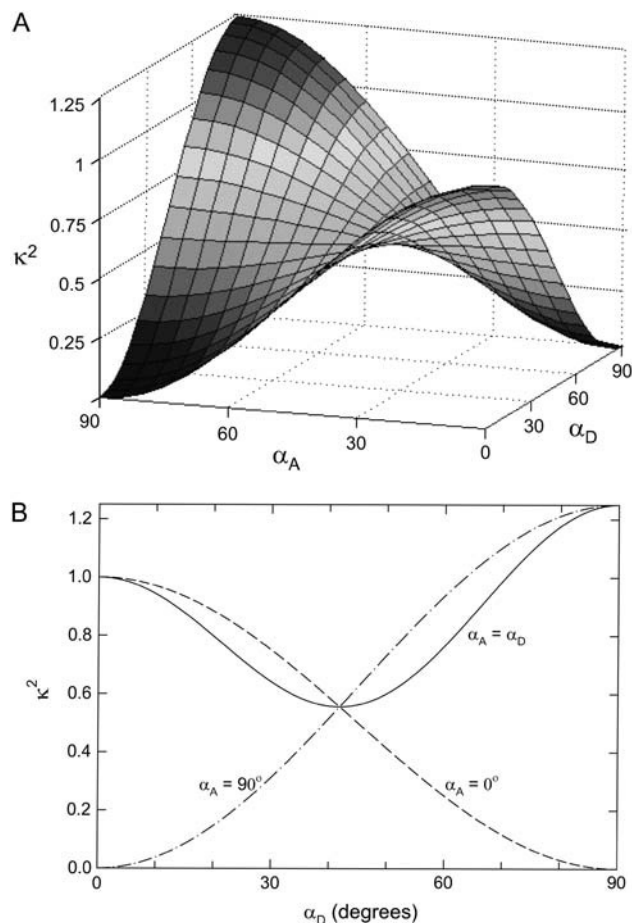

FIGURE 8 The orientation factor for transfer between independent fluorophores with known distributions. (A) The orientation factor is plotted for all possible values of the mean angle between the donor and acceptor fluorophores with the membrane normal (α_D and α_A) assuming $u = 1$. (B) The results are plotted for specific values of α_A.

The values from Eqs. 34–36 can then be substituted into Eq. 30 to calculate the orientation factor. The relationship between κ^2 and the angles α_D and α_A for independent fluorophores are plotted in Fig. 8. Fig. 8 A plots the value of the orientation factor for the full range of possible values of α_D and α_A. In Fig. 8 B, we show κ^2 for particular values of α_A.

κ^2 for fluorophores with defined relationships

If the fluorophores are attached in a defined way to a host molecule embedded in a membrane, it is likely that they will posses defined orientation to one another and the model presented above will not be valid. However, knowledge of the relationship between the fluorophores can be used to calculate explicit values for κ^2 for transfer between the fluorophores.

As previously, we can write the orientation vector of either fluorophore as

$$\mathbf{f} = \begin{pmatrix} \cos\tau \sin\alpha \\ \sin\tau \sin\alpha \\ \cos\alpha \end{pmatrix}. \qquad (37)$$

However, rather than averaging over all τ, we will let its value be dictated by the geometry of the system. For a specific value of τ,

$$\begin{aligned} \kappa^{x2} &= \left[(\mathbf{f}_D \cdot \mathbf{f}_A) - 3(\mathbf{f}_D \cdot \mathbf{x})(\mathbf{f}_A \cdot \mathbf{x}) \right]^2 \\ &= \left[-2\cos\tau_D \cos\tau_A \sin\alpha_D \sin\alpha_A \right. \\ &\quad + \sin\tau_D \sin\tau_A \sin\alpha_D \sin\alpha_A \\ &\quad \left. + \cos\alpha_D \cos\alpha_A \right]^2, \end{aligned} \qquad (38)$$

and the depolarization factors are given by Eq. 35 as before.

The simplest example of fluorophores with defined relationships is for two fluorophores attached to opposite sides of a symmetric molecule, in which case $\tau_D = \tau_A = 0$, as indicated in Fig. 7 B. In this case,

$$\kappa^{x2} = (-2\sin\alpha_D \sin\alpha_A + \cos\alpha_D \cos\alpha_A)^2. \qquad (39)$$

In our experiment, the fluorophores are attached on a pentameric protein. Thus, the projection of the mean

orientation of any fluorophore will be offset by 72° from its neighbors. In this case, there are two possible configurations that have to be taken into account: transfer between neighboring fluorophores, and transfer between next-nearest neighbors. Looking at Fig. 7 C, it can be shown that, in a pentamer, the angles τ for use in Eq. 38 will be as shown below for Eqs. 40–42.

Nearest neighbors

$$\tau_D = \frac{7\pi}{10} = 126°, \quad \tau_A = \frac{3\pi}{10} = 54°. \quad (40)$$

Next-nearest neighbors

$$\tau_D = \frac{9\pi}{10} = 162°, \quad \tau_A = \frac{\pi}{10} = 18°, \quad (41)$$

with

$$\cos\theta_D = \cos\tau_D \sin\alpha_D, \cos\theta_A = \cos\tau_A \sin\alpha_A. \quad (42)$$

It should be noted that because of the different value of τ, the value of $\langle\kappa^2\rangle$ will be different for transfer between nearest and next-nearest neighbors. The value of $\langle\kappa^2\rangle$ for various values of α_D and α_A is shown in Fig. 9 A for transfer between nearest neighbors in the pentamer. Clearly transfer is most favored when the fluorophores lie parallel to the membrane, i.e., $\alpha_D = \alpha_A = 90°$. Transfer is more favored between next-nearest neighbors than nearest neighbors as the geometry of the situation makes the transition dipoles more aligned, although the distance between them is greater. This can be seen in Fig. 9 B, where $\langle\kappa^2\rangle$ is plotted for specific values of α_A.

Example calculation for fluorophores on a pentameric protein

In Fig. 10 we plot the possible values of κ^2 for the allowed range of mean orientations α_D and α_A for our observed values of the parameters B using Eqs. 30 and 38. It is obvious that the orientation factor has its greatest value when α_D and α_A are both at the bottom end of the allowed range. The contours are much flatter when the mean orientations are further from the membrane normal.

In Table 2 we show the values of κ^2 and R_0 for transfer between the AF488 and AF568 attached to the pentameric MscL protein using the limits on the angle α and the distribution u described in Table 1. That is, we give values at the four corners of the plots shown in Fig. 10, A and B, to illustrate a range of possible κ^2 including the maximum and minimum.

It can be seen from the contour plots and Table 2 that κ^2 can adopt values over a fairly large range. However, the shape of the contour plots also suggests that for most values of α_D and α_A, κ^2 is at the lower end of the range. In Fig. 10 C
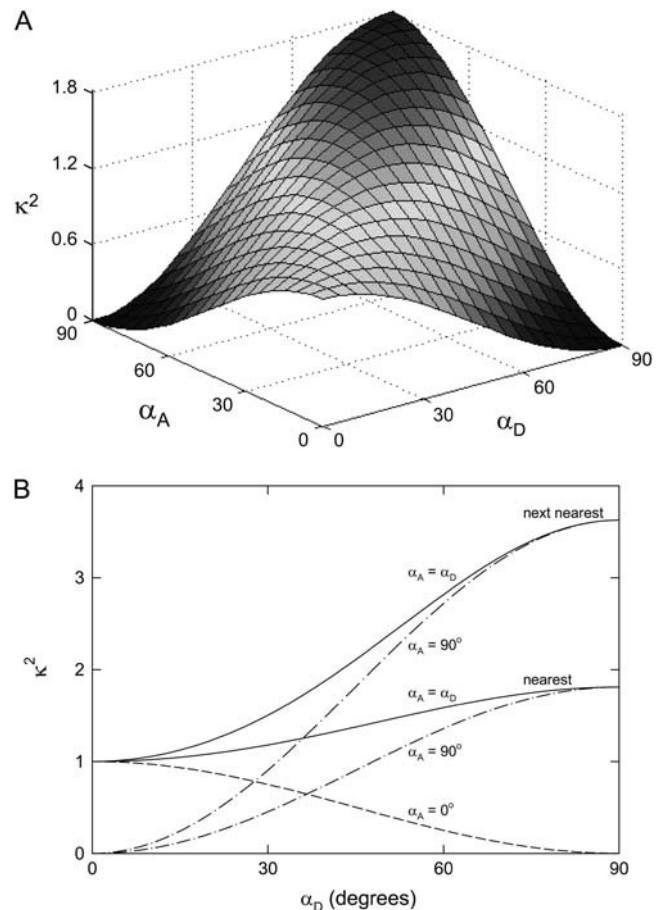

FIGURE 9 The orientation factor for transfer between fluorophores held in a pentamer. (A) The orientation factor is plotted for all possible values of the mean angle between the donor and acceptor fluorophores with the membrane normal (α_D and α_A) assuming $u = 1$ for transfer between nearest neighbors in the pentamer. (B) The results plotted for specific values of α_A for both transfer to nearest and next-nearest neighbors.

we plot the probability of κ^2 falling in an interval of size 0.005 about the specified value if all allowed values of the angles α_1 and α_2 are equally likely, as calculated from the area of a given contour in the plots shown in Fig. 10, A and B. This approach is similar to that taken by Haas et al. (32), who examined the likelihood of κ^2 falling in a given range assuming that all orientations were equally likely. In our case we are able to include the determined limits on the possible orientations, and it is clear that values at the lower end of the range are most likely. As noted by Dale et al. (6), some care should be taken when interpreting such probability plots, as the range of possible mean orientations represents our lack of knowledge of the system. In a real case, the fluorophores will have one given mean orientation that could lie anywhere on the contour plot.

Even though we are only able to determine a range of allowed values of the orientation factor κ^2, we find that if the radius of the pentamer is calculated using these values with a Monte Carlo scheme described previously (33), then the error
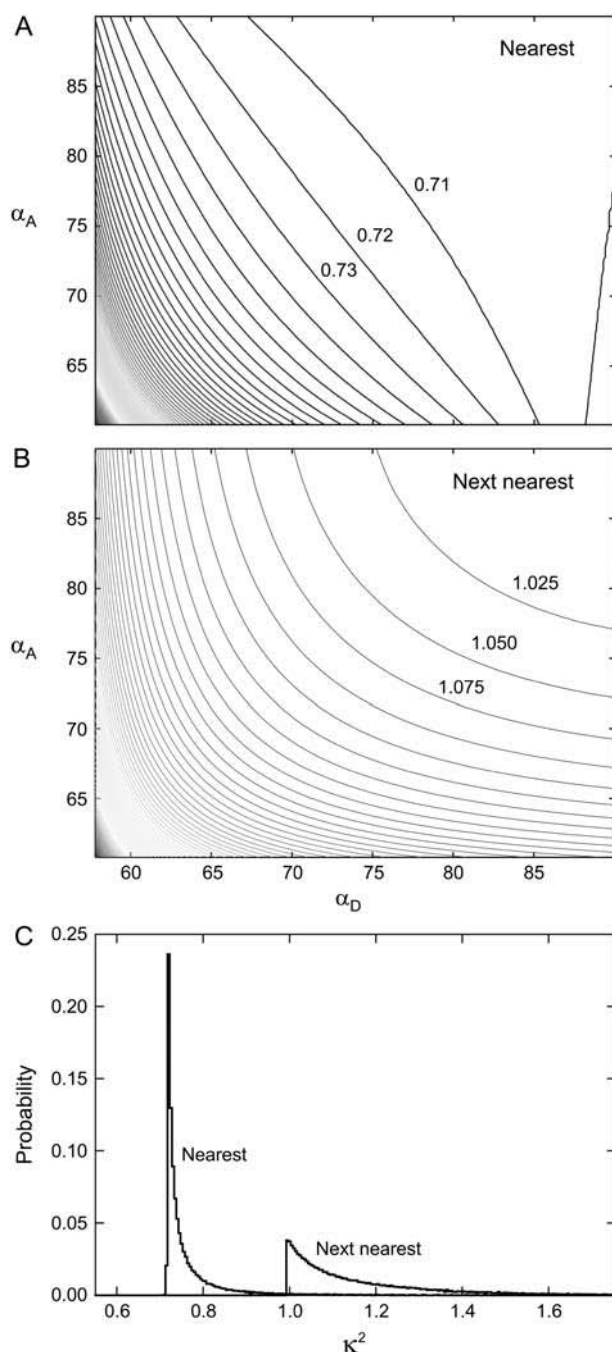
TABLE 2 Values of the orientation factor, κ^2, and the characteristic transfer distance, R_0, for transfer between the fluorophores imaged in Fig. 4

α_D	α_A	u_D	u_A	κ^2	R_0
57.8°	60.8°	1.0	1.0	1.57	71.5
				2.81	78.8
90°	60.8°	0.433	1.0	0.71	62.7
				1.28	69.1
57.8°	90°	1.0	0.525	0.78	63.6
				1.45	70.5
90°	90°	0.433	0.525	0.72	62.8
				1.00	66.3

Values are calculated for all the limiting values given in Table 1. The first row for each set of parameters is for transfer to nearest neighbors in the pentamer, and the second row is for transfer to next-nearest neighbors.

CONCLUSION

We have presented a practical scheme for determining limits on the mean orientation of membrane-bound fluorophores, as well as their orientational freedom, by imaging them with linearly polarized light in a confocal microscope. The parameter B can be obtained by fitting the intensity of emitted light as it varies with the angle of the membrane normal to the polarization of the incident light. Limits on the mean orientation of the fluorophores relative to the membrane normal, α, and the orientational freedom u can then be determined from Eqs. 20–23 assuming a cylindrically symmetric distribution of fluorophores about their mean orientation.

In our case, the fluorophores were bound to spherical liposome so that the confocal image included regions where the membrane was tilted at all angles relative to the polarization of the incident light. However, the technique need not be restricted just to membrane-bound fluorophores and can be applied to any macroscopically oriented system such as when the fluorophores are attached to a filament or surface provided that either the sample or the polarization of the incident light can be rotated without unduly altering the signal intensities passing through the detection system. We have also shown that the orientation factor, κ^2, for transfer between two fluorophores with known transition moment distributions can be obtained if some knowledge of the relative geometry is assumed.

Together the simple calculations described here provide a powerful tool. The ability to calculate the rotational freedom of fluorophores from confocal images will be of assistance for examining changes in their environment. Perhaps more important is the ability to place limits on orientation factors for use in FRET spectroscopy, which has long been plagued by uncertainty due to the ill-determined nature of this parameter.

FIGURE 10 Plots of κ^2 versus the mean fluorophore orientation for transfer AlexaFluor488 (α_D) and AlexaFluor568 (α_A) labeled to an MscL pentamer. Contours of κ^2 are indicated for all allowed values of α_1 and α_2 for transfer between nearest neighbors (A) and next-nearest neighbors (B). Contour intervals are 0.01 in panel A and 0.025 in panel B. The probability of obtaining κ^2 in intervals of width 0.005 is plotted in panel C as obtained from the areas of the contour plots.

in radius is relatively small. The uncertainties are even smaller if changes in distance are being determined; as in this case, the distances are related to the slope of the efficiency of energy transfer (refer back to Eq. 1) rather than the exact values.

REFERENCES

1. Badley, R. A., W. G. Martin, and H. Schneider. 1973. Dynamic behavior of fluorescent probes in lipid bilayer model membranes. *Biochemistry.* 12:268–275.

2. Kawato, S., K. Jr. Kinosita, and A. Ikegami. 1977. Dynamic structure of lipid bilayers studied by nanosecond fluorescence techniques. *Biochemistry.* 31:2319–2324.

3. Lakowicz, J. R. 1999. Principles of Fluorescence Spectroscopy, 2nd Ed. Kluwer, New York.

4. Michl, J., and E. W. Thulstrup. 1986. Spectroscopy with Polarized Light. VCH, New York.

5. Kubista, M., B. Åkerman, and B. Albinsson. 1989. Characterization of the electronic structure of 4′6-diamidino-2-phenylindole. *J. Am. Chem. Soc.* 111:7031–7035.

6. Dale, R. E., J. Eisinger, and W. E. Blumberg. 1979. The orientational freedom of molecular probes: the orientation factor in intramolecular energy transfer. *Biophys. J.* 26:161–194.

7. van der Meer, B. W., R. P. H. Kooyman, and Y. K. Levine. 1982. A theory of fluorescence depolarization in macroscopically ordered membrane systems. *Chem. Phys.* 66:39–50.

8. van Gurp, M., H. van Langen, G. van Ginkel, and Y. K. Levine. 1988. Angle-resolved techniques in studies of organic molecules in ordered systems using polarized light. *In* Polarized Spectroscopy of Ordered Systems. B. Samorí and E. W. Thulstrup, editors. Kluwer, Dordrecht, The Netherlands.

9. van der Heide, U. A., B. Orbons, H. C. Gerritsen, and Y. K. Levine. 1992. The orientation of transition moments of dye molecules used in fluorescence studies of muscle systems. *Eur. Biophys. J.* 21:263–272.

10. van der Heide, U. A., O. E. Rem, H. C. Gerritsen, E. L. de Beer, P. Schiereck, I. P. Taylor, and Y. K. Levine. 1994. A fluorescence depolarization study of the orientational distribution of crossbridges in muscle fibres. *Eur. Biophys. J.* 23:369–378.

11. Blackman, S. M., C. E. Cobb, A. H. Beth, and D. W. Piston. 1996. The orientation of eosin-5-maleimide on human erythrocyte band 3 measured by fluorescence polarization microscopy. *Biophys. J.* 71:194–208.

12. Benninger, R. K. P., B. Önfelt, M. A. A. Neil, D. M. Davis, and P. M. W. French. 2005. Fluorescence imaging of two-photon linear dichroism: cholesterol depletion disrupts molecular orientation in cell membranes. *Biophys. J.* 88:609–622.

13. Rocheleau, J. V., M. Edidin, and D. W. Piston. 2003. Intrasequence GFP in class 1 MHC molecules, a rigid probe for fluorescence anisotropy measurements of the membrane environment. *Biophys. J.* 84:4078–4086.

14. Weiss, S. 2000. Measuring conformational dynamics of biomolecules by single molecule fluorescence spectroscopy. *Nat. Struct. Biol.* 7:724–729.

15. Rasnik, I., S. A. McKinney, and T. Ha. 2005. Surfaces and orientations: much to FRET about? *Acc. Chem. Res.* 38:542–548.

16. Adachi, K., R. Yasuda, H. Noji, H. Itoh, Y. Harada, M. Yoshida, and K. Kinosita, Jr. 2000. Stepping rotation of F1-ATPase visualized through angle-resolved single-fluorophore imaging. *Proc. Natl. Acad. Sci. USA.* 97:7243–7247.

17. Rothwell, P. J., S. Berger, O. Kensch, S. Felekyan, M. Antonik, B. M. Whrl, T. Restle, R. S. Goody, and C. A. M. Seidel. 2003. Multiparameter single-molecule fluorescence spectroscopy reveals heterogeneity of HIV-1 reverse transcriptase:primer/template complexes. *Proc. Natl. Acad. Sci. USA.* 100:1655–1660.

18. Förster, T. 1959. Transfer mechanisms of electronic excitation. *Discuss. Faraday Soc.* 27:7–17.

19. Van Der Meer, B. W., G. Coker, and S. Y. S. Chen. 1994. Resonance Energy Transfer: Theory and Data. VCH, New York.

20. Clegg, R. M. 1996. Fluorescence resonance energy transfer (FRET). *In* Fluorescence Imaging Spectroscopy and Microscopy. X. F. Wang and B. Herman, editors. Wiley and Sons, New York. 179–252.

21. Jares-Erijman, E. A., and T. M. Jovin. 2003. FRET imaging. *Nat. Biotechnol.* 21:1387–1395.

22. Dos Remedios, C. G., and P. D. J. Moens. 1995. Fluorescence resonance energy transfer spectroscopy is a reliable ''ruler'' for measuring structural changes in proteins. *J. Struct. Biol.* 115:175–185.

23. Dale, R. E., and J. Eisinger. 1974. Intermolecular distances determined by energy transfer. Dependence on orientational freedom of donor and acceptor. *Biopolymers.* 13:1573–1605.

24. Blumberg, W. E., R. E. Dale, J. Eisinger, and D. M. Zuckerman. 1974. Energy transfer in tRNA^{PHE} (Yeast). The solution structure of transfer RNA. *Biopolymers.* 13:1607–1620.

25. Haas, E., E. Katchalski-Katzir, and I. Z. Steinberg. 1978. Effect of the orientation of donor and acceptor on the probability of energy transfer involving electronic transitions of mixed polarization. *Biochemistry.* 17:5064–5070.

26. Saccá, B., S. Fiori, and L. Moroder. 2003. Studies of the local conformational properties of the cell-adhesion domain of collagen type IV in synthetic heterotrimeric peptides. *Biochemistry.* 42:3429–3436.

27. Stryer, L., and R. P. Haugland. 1967. Energy transfer: spectroscopic ruler. *Proc. Natl. Acad. Sci. USA.* 58:716–726.

28. Stryer, L. 1978. Fluorescence energy transfer as a spectroscopic ruler. *Annu. Rev. Biochem.* 47:819–846.

29. Kloda, A., and B. Martinac. 2001. Molecular identification of a mechanosensitive channel in archaea. *Biophys. J.* 80:229–240.

30. Häse, C. C., A. C. LeDain, and B. Martinac. 1995. Purification and functional reconstitution of the recombinant large mechanosensitive ion channel (MscL) of *Escherichia coli. J. Biol. Chem.* 270:18329–18334.

31. Eisinger, J., and R. E. Dale. 1974. Interpretation of intramolecular energy transfer experiments. *J. Mol. Biol.* 84:643–647.

32. Haas, E., E. Katchalski-Katzir, and I. Z. Steinberg. 1975. Effect of the orientation of donor and acceptor on the probability of energy transfer involving electronic transitions of mixed polarization. *Biochemistry.* 17:5065–5070.

33. Corry, B., D. Jayatilaka, and P. Rigby. 2005. A flexible approach to the calculation of resonance energy transfer efficiency between multiple donors and acceptors in complex geometries. *Biophys. J.* 89:3822–3836.